FEBS Letters 586 (2012) 1344–1348

journal homepage: www.FEBSLetters.org

Kinetics of proton release and uptake by channelrhodopsin-2

Melanie Nack [a], Ionela Radu [a], Bernd-Joachim Schultz [a], Tom Resler [a], Ramona Schlesinger [a], Ana-Nicoleta Bondar [a], Coral del Val [b], Stefania Abbruzzetti [c], Cristiano Viappiani [c], Christian Bamann [d], Ernst Bamberg [d], Joachim Heberle [a,*]

[a] Freie Universität Berlin, Institute for Experimental Physics, Arnimallee 14, 14195 Berlin, Germany
[b] University of Granada, Department of Computer Science and Artificial Intelligence, E-18071, Spain
[c] Università degli Studi di Parma, Dipartimento di Fisica, 43100 Parma, Italy
[d] Max-Planck-Institute for Biophysics, Max-von-Laue-Straße 3, 60438 Frankfurt am Main, Germany

ARTICLE INFO

Article history:
Received 15 March 2012
Accepted 23 March 2012
Available online 6 April 2012

Edited by Peter Brzezinski

Keywords:
Bacteriorhodopsin
Proton transfer
Optogenetics
Rhodopsin
Ion channel

ABSTRACT

Electrophysiological experiments showed that the light-activated cation channel channelrhodopsin-2 (ChR2) pumps protons in the absence of a membrane potential. We determined here the kinetics of transient pH change using a water-soluble pH-indicator. It is shown that ChR2 released protons prior to uptake with a stoichiometry of 0.3 protons per ChR2. Comparison to the photocycle kinetics revealed that proton release and uptake match rise and decay of the P_3^{520} intermediate. As the P_3^{520} state also represents the conductive state of cation channeling, the concurrence of proton pumping and channel gating implies an intimate mechanistic link of the two functional modes. Studies on the E123T and S245E mutants show that these residues are not critically involved in proton translocation.

1. Introduction

Optogenetics is a vibrant field where light-sensitive proteins are targeted to induce specific physiological responses in living cells and organisms with high spatio-temporal resolution [1]. The recently identified light-gated ion channel channelrhodopsin-2 (ChR2) [2] became a versatile tool to activate neuronal cells by light [3]. Despite the large number of optogenetic applications of ChR2, the functional mechanism of this protein is largely unknown on the molecular level. The structural model of ChR2 based on a 6 Å cryo-electron microscopy projection map showed that the arrangement of the transmembrane helices is similar to bacteriorhodopsin [4]. It was inferred from the dimeric structure of ChR2 that helices C and D are critically involved in ion channeling as corroborated by functional studies on point mutants (DC gate) [5]. Recently, the crystal structure of a chimaera of channelrhodopsin was determined to a resolution of 2.3 Å [6] and confirmed the dimeric arrangement of the monomers. However, the high-resolution data together with functional assessments favored helices A, B, C, and G as cation-conducting pathway.

The photoreaction of ChR2 is reminiscent to other microbial rhodopsins, albeit more intricate [7–9]. Spectroscopic and electrophysiological data revealed that the cation flow is correlated to the kinetics of the red-shifted P_3^{520} state but recent studies on ChR2 mutants suggest that the preceding blue-shifted P_2^{390} state might be conductive as well [10]. It was concluded from FT-IR difference spectroscopic experiments that the protein backbone undergoes large conformational changes after photoactivation of ChR2 [11,12] but that opening of the gate of the ion channel is restricted only to the movement of several unidentified amino acids [12]. Closing of the gate coinciding with the transition from the P_3^{520} state to the desensitized P_4^{480} state, is coupled to only small protein distortions.

ChR2 belongs to the large family of microbial rhodopsins that also includes ion pumps and light sensors [13]. Compelling evidence showed that sensory rhodopsins are capable to pump protons although with low efficiency [14,15]. Feldbauer et al. [16] reported the remarkable observation that ChR2 acts not only as a channel but also exhibits proton pumping activity. However, the mechanistic relationship between proton pumping and ion channeling is not clear. The experiments by Feldbauer et al. [16] could not correlate the observed proton translocation activity to the kinetics of the photoreaction. For this goal, we monitored here the time-dependent proton translocation in ChR2 using a pH-indicating dye. This approach has been successfully employed to determine the kinetics of proton release and uptake in bacteriorhodopsin (BR) [17–19]. We show here that ChR2 releases protons in the early millisecond domain concurrent with the rise of the P_3^{520} state. The uptake of

* Corresponding author. Address: Freie Universität Berlin, Experimental Molecular Biophysics, Arnimallee 14, D-14195 Berlin, Germany. Fax: +49 30 838 56510.
E-mail address: joachim.heberle@fu-berlin.de (J. Heberle).

0014-5793/$36.00
http://dx.doi.org/10.1016/j.febslet.2012.03.047

protons proceeds bi-phasic reflecting the equilibrium between the late P_3^{520} and P_4^{480} states. As the P_3^{520} state is characterized by the retinal owing a protonated Schiff base, this finding contrasts bacteriorhodopsin where proton release is coupled to the deprotonation of the Schiff base. Studies of the E123T and S245E mutants agree with the conclusion that ChR2 is a proton pump but with mechanistic deviations from prototypic bacteriorhodopsin. However, ChR2 is a poor proton pump as indicated by the stoichiometry of 0.3 protons released per photocycling ChR2.

2. Materials and methods

Channelrhodopsin-2 (ChR2) and the point mutants E123T and S245E [5] were heterologously expressed in the yeast *Pichia pastoris* [12]. The wild-type and mutant proteins were purified by Ni-NTA affinity chromatography using 250 mM imidazole as the eluent. For the time-resolved UV/Vis experiments, 15 μM ChR2 (dissolved in 0.2% decyl maltoside, 100 mM NaCl, pH 7.4) were excited by a short pulse from a solid-state laser (Nd:YAG driven OPO, 10 ns laser pulse at 475 nm, energy density of 4 mJ/cm^2, one pulse every minute) and the absorption changes detected by a photomultiplier were recorded on a quasi-logarithmic time-scale from 100 ns to 50 s. The measuring light was the emission from either a HeNe laser (in the laboratory in Parma) or from a halogen bulb passing a monochromator set to the desired wavelength (Berlin laboratory). The optical pH indicator bromoxylenol blue (15 μM BXB) was used for detection of transient pH changes in the aqueous solution. Prior to the time-resolved pH indicator experiments, great care was taken to completely remove the imidazole buffer by repetitive washing steps and centrifugation of the solution through polycarbonate filters (Amicon Ultra Centrifugal Filter, cut-off 50 kDa). Multi-exponential fits to the kinetic traces have been obtained with the Levenberg–Marquardt algorithm.

3. Results and discussion

Fig. 1 represents the absorption changes of the water-soluble pH indicator bromoxylenol blue (BXB) after pulsed laser excitation of ChR2 [20]. The transients have been recorded at a wavelength of 620 nm which corresponds to the maximum absorption of the deprotonated form of BXB. ChR2 did not exhibit any photo-induced absorption changes at this long wavelength. The absorption changes displayed in Fig. 1 were negative which indicates transient pH drop in the solution, i.e., proton release by ChR2. The stepwise addition of HEPES buffer (resulting in final concentrations of 100 μM, 250 μM, or 400 μM HEPES, Fig. 1A) decreased the amplitude of the transient BXB signal. At even higher buffer concentrations (14 mM), the response of BXB completely disappeared (not shown). The disappearance of the signal demonstrates that the observed transient absorption changes are exclusively caused by proton transfer reactions rather than by solvatochromism of protein bound dye.

The magnitude of the transient absorbance change of the pH-indicator BXB was titrated with calibrated amounts of protons (by the addition of HCl). Based on the number of ChR2 molecules undergoing the photocycle (9% under our conditions of laser excitation), a stoichiometry of 0.3 ± 0.1 H^+/ChR2 was determined. The comparison to BR which pumps one proton per photocycling molecule, indicates that ChR2 is not very efficient in proton pumping. It is noted that the proton release stoichiometry of 0.3 agrees well with an estimate of 0.2–0.4 elementary charges pumped by ChR2 derived independently from electrophysiology [16]. Thus, our results substantiate the idea that the light-gated cation channel ChR2 has residual proton pumping activity.

To correlate the observed proton transfer reactions to the appearance of photocycle intermediates of ChR2, we recorded the rise and decay of the P_2^{390} (upper trace in Fig. 2) and the P_3^{520} states (middle trace). The comparison of the time course of the respective photocycle intermediate to the BXB signal indicated that the kinetics of the pH indicator matched those of the P_3^{520} state. The rise of the preceding P_2^{390} state was much faster (τ = 10 μs, top trace). As the rise of the P_2^{390} state reflects Schiff base deprotonation (step 1 in Fig. 3B), it is obvious that the latter did not lead to immediate proton release into the surrounding aqueous phase. Such delay between Schiff base deprotonation and proton release into the aqueous bulk has also been observed for BR solubilized in detergent micelles [21]. However, proton release by solubilized BR proceeded with a time constant of 110 μs which is one order of magnitude faster than proton release of solubilized ChR2 (τ = 1.7 ms, bottom trace of Fig. 2). Mobile buffer molecules like HEPES are able to

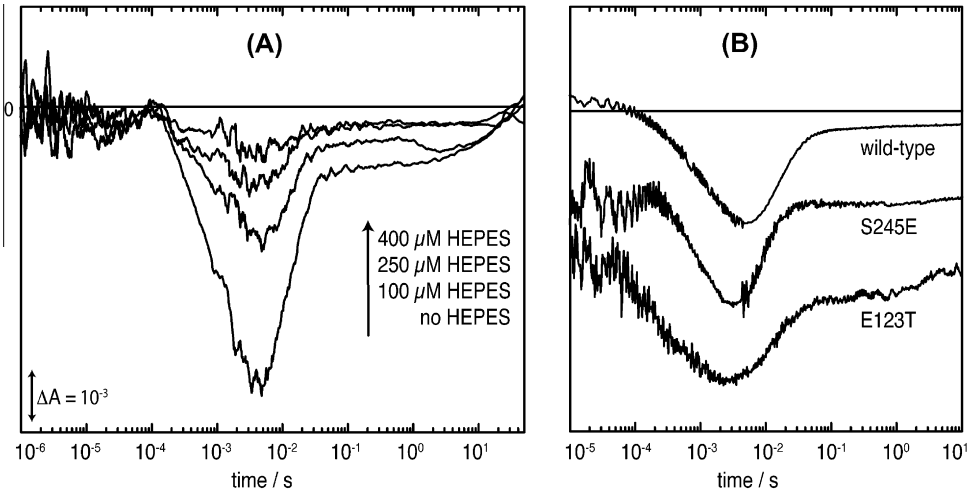

Fig. 1. (A) Transient pH changes in the aqueous solution of detergent-solubilized channelrhodopsin-2 (ChR2) detected by the optical pH indicator bromoxylenol blue (15 μM BXB) at 620 nm. 15 μM ChR2 (dissolved in 0.2% decyl maltoside, 100 mM NaCl, pH 7.4, 20 °C) were excited by a 10 ns pulse from a tunable solid-state laser (Nd:YAG driven OPO, 10 ns laser pulse at 475 nm, energy density of 4 mJ/cm^2, one pulse every minute). Downward deflections of the kinetic traces indicate transient decrease in pH corresponding to proton release by ChR2. The BXB transients were recorded in the absence (no HEPES, lowest trace) and in the presence of various concentrations of HEPES buffer as indicated. (B) Proton release and uptake in the E123T and the S245E mutants monitored by BXB. The kinetic traces are offset along the *y*-axis for clarity. The trace of wild-type ChR2 is depicted for comparison, which was recorded in an independent experiment as in panel A but under the same conditions.

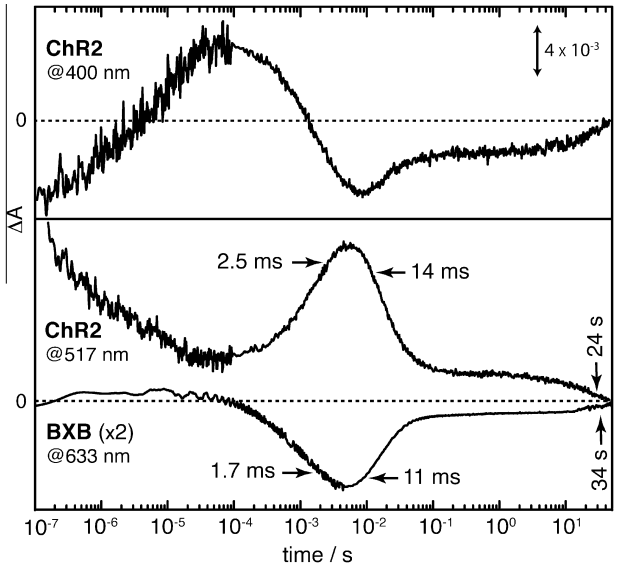

Fig. 2. Comparison of the photocycle kinetics of ChR2 recorded at 400 nm (top trace) and at 517 nm (middle trace) and of the pH changes monitored by BXB (bottom trace). Arrows indicate the calculated time constants from multi-exponential fits to the kinetic traces. The absorbance changes of the pH indicator BXB were monitored at 633 nm using the emission of a HeNe laser [41] and are magnified by a factor of 2 in amplitude. All other conditions are the same as described in Fig. 1.

act as proton shuttles and accelerate the (apparent) proton diffusion from the protein surface to the aqueous bulk solution [22]. Time-resolved experiments recorded in the presence of micromolar concentrations of HEPES (Fig. 1A) showed that the time course of proton release by ChR2 is independent of the presence of HEPES buffer. These results rule out the response time of BXB being limited by the transfer of protons from the membrane surface to the bulk aqueous phase. Rather, our experiments provide evidence that the BXB signal reflects intraproteinous proton transfer to the membrane surface (step 3 in Fig. 3B) that takes place during the rise of the red-shifted P_3^{520} state (τ = 2.5 ms). This conclusion is surprising given the fact that the retinal Schiff base is (re-)protonated in the P_3^{520} state (step 2 in Fig. 3B) [12]. In contrast, proton release by BR (step 2 in Fig. 3A) is closely linked to the deprotonation of the Schiff base.

The primary proton acceptor of the Schiff base proton in BR is D85. Exchange of D85 to any non-protonatable residue lead to the malfunction of proton pumping activity in BR [23–25]. The D85T mutation even converted BR into a chloride pump [26]. Thus, we exchanged the homologous residue in ChR2, E123, to threonine expecting that the kinetics of proton release and/or uptake are strongly impaired. However, the response of BXB clearly indicated proton release after photo-excitation of the E123T mutant with kinetics similar to the wild type (Fig. 1B). A slightly accelerated proton release reaction is noted though (about twice as fast in the mutant than in the wild type). These observations indicate that the mechanism of proton release by ChR2 must be different to BR where protonation of D85 (step 1 in Fig. 3A) triggers immediate proton release from the proton release complex into the aqueous bulk phase (step 2 in Fig. 3A) [19].

As demonstrated by the transient pH indicator experiments (Fig. 1), proton release precedes proton uptake in ChR2. Such early proton release was also observed in BR at neutral and alkaline pH. The proton release complex of BR is comprised of a hydrogen-bonded network that includes the dyad E194/E204 at the extracellular surface (Fig. 3) and several water molecules accommodating an excess proton. Studies on BR mutants lacking these carboxylic side chains inferred that the early proton release is associated with

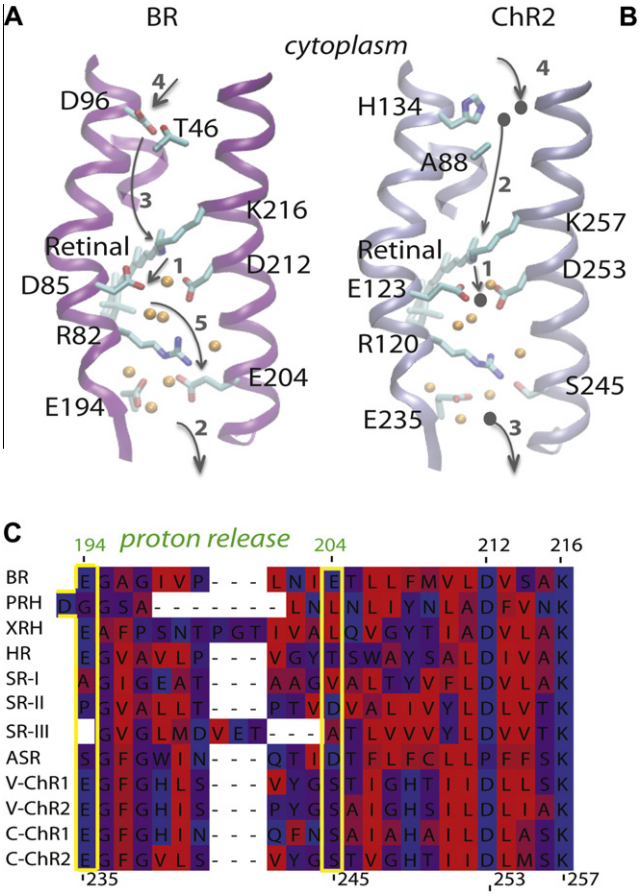

Fig. 3. Putative proton transfer paths and their temporal sequence in BR and ChR2. (A, B) Schematic representations of BR (panel A) and ChR2 (panel B) with helices shown as green ribbons, water molecules as orange spheres, and retinal and selected amino acids shown as bonds. Arrows with numbers denote proton transfer steps derived from FT-IR and flash photolysis data. The gray filled circles in panel B indicate that the identity of the proton donor/acceptor group is unknown. As a first approximation, the structural model of ChR2 was generated by replacing BR amino acids T46, D85, D96, and E204 with the corresponding ones in ChR2, and performing a geometry optimization using the CHARMM software [42]. (C) Sequence alignment of microbial rhodopsins showing the proton release (panel C) region of BR-E194/E204. Note that neither BR-E194 nor BR-E204 are absolutely conserved. In channelrhodopsins, BR-E194 and BR-E204 are present as Glu and Ser, respectively. Amino acids are colored according to the Kyte and Doolittle scheme [43] from red (most hydrophobic) to blue (most hydrophilic). The following abbreviations are used: BR – bacteriorhodopsin; PRH – proteorhodopsin; XRH – xanthorhodopsin; HR – halorhodopsin; SR-I, SR-II, and SR-III: sensory rhodopsins I, II and III; ASR – anabaena sensory rhodopsin; V-CHR1, V-CHR2: channelrhodopsins 1 and 2 from *V. carteri*; C-CHR1, C-CHR2: channelrhodopsins 1 and 2 from *C. reinharditii*. The sequences and structures of BR, HR, SR-II, and XRH used to construct the alignment were extracted from the protein data bank. T-Coffee [44] and ClustalW [45] were used for sequence alignments. Molecular graphics images were prepared with the VMD software [46]. The complete sequence alignment is available under: www.physik.fu-berlin.de/en/einrichtungen/ag/ag-bondar/publications/index.html.

an intact proton release complex (i.e., the Glu dyad) [27,28]. This bold conclusion is, however, challenged by the fact that many other microbial rhodopsins, like sensory rhodopsins I and II [14,15], proteorhodopsin [29] and xanthorhodopsin [30] mediate early proton release although they lack either one of the two carboxylic residues or both. Sequence alignment shows that E204 of BR is replaced by a serine residue in ChR2 (S245) and other channelrhodopsins, whereas E194 is conserved (Fig. 3C). In an attempt to re-install the carboxylic dyad, we designed the S245E mutant of ChR2 and expressed the protein variant. Time-resolved spectroscopy showed, however, that neither the kinetics of the photocycle nor that of proton release is altered by the amino acid exchange

(Fig. 1B). These results suggest that S245 is not a critical part of the proton release group. In general terms, our results raise anew the question as to whether an intact proton release group (i.e., containing a Glu dyad) is indeed a prerequisite for early proton release in microbial rhodopsins. Based on the results presented here and by Brown and Jung [31], we conclude that the carboxylate dyad at the homolog positions 194 and 204 of BR is not a prerequisite to early proton release.

Protons are taken up by ChR2 in two phases that are separated by more than three orders of magnitude in time (τ = 11 ms and 34 s, bottom trace in Fig. 2). The deprotonation reaction of BXB matches the decay kinetics of the P_3^{520} state (τ = 14 ms and 24 s, middle trace). The fact that proton uptake is biphasic can be readily explained by an equilibrium between the P_3^{520} and P_4^{480} states. Proton uptake (step 4 in Fig. 3B) is concurrent with critical conformational changes within the protein. Indeed, our earlier FT-IR data showed that the P_3^{520} decay to the ground state (via P_4^{480}) is associated with retinal back-isomerization as well as large protein rearrangements [12] which are processes demanding high energetic costs [32]. Proton uptake in BR (step 4 in Fig. 3A) involves protonation reactions of a cytoplasmic cluster of carboxylic amino acids (proton antenna) [33–35] that extend to D96 which acts as internal proton donor of the retinal Schiff base [36,37]. D96 is replaced by H134 in ChR2 (Fig. 3B), a replacement that is conserved in all ChR sequences analyzed here. In BR, D96 forms an inter-helical hydrogen bond with T46 [38]. This interaction is abolished in ChR2 as T46 is replaced by A88. Based on these observations we suggest that the mechanisms of the proton uptake by ChR2 and BR are different.

In conclusion, our findings demonstrate that ChR2 exhibits light-driven proton release and uptake, providing the recently reported proton pump activity of ChR2 [16] with a time line (Fig. 4). It was also shown that residues E123 and S245 are not members of the proton release pathway. Our time-resolved experiments with the pH-indicating dye BXB demonstrate that proton release precedes proton uptake in ChR2 which is similar to BR at neutral and alkaline pH. In addition to the low proton translocation efficiency of 0.3 protons per ChR2, a major mechanistic difference to BR is the fact that proton release by ChR2 occurs with the re-protonation of the retinal Schiff base (rise of the P_3^{520} state) and not with deprotonation of the latter as in BR. However, as long as detailed structural information is missing on the central P_3^{520} state, the mechanistic interplay of the pumping and the channeling activities remains elusive. It must be clearly stated at this point that our pH-indicator experiments were performed with ChR2 solubilized in detergent. The absence of a vesicular compartment impedes a direct measurement of the proton pumping activity. However, the correlation of electrophysiological experiments (which provide evidence for proton pumping) to spectroscopy was previously demonstrated for bacteriorhodopsin [39]. In the future, it will be important to determine the temporal and spatial sequence of proton transfer events within ChR2. Such time-resolved step-scan FT-IR difference spectroscopic experiments [40] are currently underway. These experiments will not only delineate the proton pathway but will help to determine the relationship between proton transfer and ion channeling.

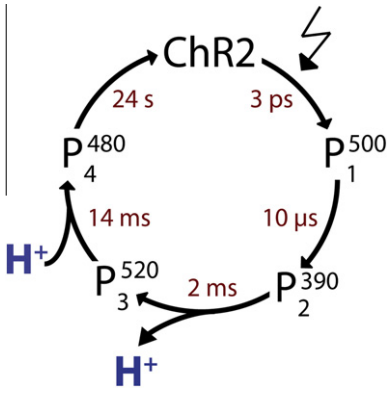

Fig. 4. Unidirectional photocycle of ChR2 including the steps at which protons are released into and taken up from the aqueous bulk phase as determined in the present work. The time constants of the transitions of the intermediate states (red) have been measured in this work (see Fig. 2) except the time constant of the rise of the $P1^{500}$ intermediate which was taken from Verhoefen et al. [47]. The equilibrium between the P_3^{520} and P_4^{480} states as identified by our experiments (see Fig. 2) has been omitted for clarity.

Acknowledgments

We thank M. Gossing and G. Fischer von Mollard (Bielefeld University, Germany) for constructing the S245E mutation. A.-N.B. is supported by the Marie Curie International Reintegration Award IRG-276920.

References

[1] Deisseroth, K. (2011) Optogenetics. Nat. Methods 8, 26–29.
[2] Nagel, G., Szellas, T., Huhn, W., Kateriya, S., Adeishvili, N., Berthold, P., Ollig, D., Hegemann, P. and Bamberg, E. (2003) Channelrhodopsin-2, a directly light-gated cation-selective membrane channel. Proc. Natl. Acad. Sci. U.S.A. 100, 13940–13945.
[3] Bamann, C., Nagel, G. and Bamberg, E. (2010) Microbial rhodopsins in the spotlight. Curr. Opin. Neurobiol. 20, 610–616.
[4] Muller, M., Bamann, C., Bamberg, E. and Kuhlbrandt, W. (2011) Projection structure of channelrhodopsin-2 at 6 a resolution by electron crystallography. J. Mol. Biol. 414, 86–95.
[5] Nack, M., Radu, I., Gossing, M., Bamann, C., Bamberg, E., von Mollard, G.F. and Heberle, J. (2010) The DC gate in channelrhodopsin-2: crucial hydrogen bonding interaction between C128 and D156. Photochem. Photobiol. Sci. 9, 194–198.
[6] Kato, H.E., Zhang, F., Yizhar, O., Ramakrishnan, C., Nishizawa, T., Hirata, K., Ito, J., Aita, Y., Tsukazaki, T., Hayashi, S., Hegemann, P., Maturana, A.D., Ishitani, R., Deisseroth, K. and Nureki, O. (2012) Crystal structure of the channelrhodopsin light-gated cation channel. Nature 482, 369–374.
[7] Bamann, C., Kirsch, T., Nagel, G. and Bamberg, E. (2008) Spectral characteristics of the photocycle of channelrhodopsin-2 and its implication for channel function. J. Mol. Biol. 375, 686–694.
[8] Ernst, O.P., Sanchez Murcia, P.A., Daldrop, P., Tsunoda, S.P., Kateriya, S. and Hegemann, P. (2008) Photoactivation of channelrhodopsin. J. Biol. Chem. 283, 1637–1643.
[9] Berndt, A., Prigge, M., Gradmann, D. and Hegemann, P. (2010) Two open states with progressive proton selectivities in the branched channelrhodopsin-2 photocycle. Biophys. J. 98, 753–761.
[10] Bamann, C., Gueta, R., Kleinlogel, S., Nagel, G. and Bamberg, E. (2010) Structural guidance of the photocycle of channelrhodopsin-2 by an interhelical hydrogen bond. Biochemistry 49, 267–278.
[11] Ritter, E., Stehfest, K., Berndt, A., Hegemann, P. and Bartl, F.J. (2008) Monitoring light-induced structural changes of channelrhodopsin-2 by UV-visible and Fourier transform infrared spectroscopy. J. Biol. Chem. 283, 35033–35041.
[12] Radu, I., Bamann, C., Nack, M., Nagel, G., Bamberg, E. and Heberle, J. (2009) Conformational changes of channelrhodopsin-2. J. Am. Chem. Soc. 131, 7313–7319.
[13] Sharma, A.K., Spudich, J.L. and Doolittle, W.F. (2006) Microbial rhodopsins: functional versatility and genetic mobility. Trends Microbiol. 14, 463–469.
[14] Olson, K.D. and Spudich, J.L. (1993) Removal of the transducer protein from sensory rhodopsin I exposes sites of proton release and uptake during the receptor photocycle. Biophys. J. 65, 2578–2585.
[15] Kitade, Y., Furutani, Y., Kamo, N. and Kandori, H. (2009) Proton release group of pharaonis phoborhodopsin revealed by ATR-FTIR spectroscopy. Biochemistry 48, 1595–1603.
[16] Feldbauer, K., Zimmermann, D., Pintschovius, V., Spitz, J., Bamann, C. and Bamberg, E. (2009) Channelrhodopsin-2 is a leaky proton pump. Proc. Natl. Acad. Sci. U.S.A. 106, 12317–12322.
[17] Lozier, R.H., Bogomolni, R.A. and Stoeckenius, W. (1975) Bacteriorhodopsin: a light-driven proton pump in Halobacterium Halobium. Biophys. J. 15, 955–962.
[18] Grzesiek, S. and Dencher, N.A. (1986) Time-course and stoichiometry of light-induced proton release and uptake during the photocycle of bacteriorhodopsin. FEBS Lett. 208, 337–342.
[19] Heberle, J. and Dencher, N.A. (1992) Surface-bound optical probes monitor proton translocation and surface potential changes during the bacteriorhodopsin photocycle. Proc. Natl. Acad. Sci. U.S.A. 89, 5996–6000.
[20] Viappiani, C., Bonetti, G., Carcelli, M., Ferrari, F. and Sternieri, A. (1998) Study of proton transfer processes in solution using the laser induced pH-jump: a

new experimental setup and an improved data analysis based on genetic algorithms. Rev. Sci. Instrum. 69, 270–276.
[21] Scherrer, P., Alexiev, U., Marti, T., Khorana, H.G. and Heyn, M.P. (1994) Covalently bound pH-indicator dyes at selected extracellular or cytoplasmic sites in bacteriorhodopsin. 1. Proton migration along the surface of bacteriorhodopsin micelles and its delayed transfer from surface to bulk. Biochemistry 33, 13684–13692.
[22] Junge, W. and McLaughlin, S. (1987) The role of fixed and mobile buffers in the kinetics of proton movement. Biochim. Biophys. Acta 890, 1–5.
[23] Mogi, T., Stern, L.J., Marti, T., Chao, B.H. and Khorana, H.G. (1988) Aspartic acid substitutions affect proton translocation by bacteriorhodopsin. Proc. Natl. Acad. Sci. U.S.A. 85, 4148–4152.
[24] Otto, H., Marti, T., Holz, M., Mogi, T., Stern, L.J., Engel, F., Khorana, H.G. and Heyn, M.P. (1990) Substitution of amino acids Asp-85, Asp-212, and Arg-82 in bacteriorhodopsin affects the proton release phase of the pump and the pK of the Schiff base. Proc. Natl. Acad. Sci. U.S.A. 87, 1018–1022.
[25] Tittor, J., Haupts, U., Haupts, C., Oesterhelt, D., Becker, A. and Bamberg, E. (1997) Chloride and proton transport in bacteriorhodopsin mutant D85T: different modes of ion translocation in a retinal protein. J. Mol. Biol. 271, 405–416.
[26] Sasaki, J., Brown, L.S., Chon, Y.S., Kandori, H., Maeda, A., Needleman, R. and Lanyi, J.K. (1995) Conversion of bacteriorhodopsin into a chloride ion pump. Science 269, 73–75.
[27] Brown, L.S., Sasaki, J., Kandori, H., Maeda, A., Needleman, R. and Lanyi, J.K. (1995) Glutamic acid 204 is the terminal proton release group at the extracellular surface of bacteriorhodopsin. J. Biol. Chem. 270, 27122–27126.
[28] Dioumaev, A.K., Richter, H.T., Brown, L.S., Tanio, M., Tuzi, S., Saito, H., Kimura, Y., Needleman, R. and Lanyi, J.K. (1998) Existence of a proton transfer chain in bacteriorhodopsin: participation of Glu-194 in the release of protons to the extracellular surface. Biochemistry 37, 2496–2506.
[29] Krebs, R.A., Alexiev, U., Partha, R., DeVita, A.M. and Braiman, M.S. (2002) Detection of fast light-activated H+ release and M intermediate formation from proteorhodopsin. BMC Physiol. 2, 5.
[30] Balashov, S.P., Imasheva, E.S., Boichenko, V.A., Anton, J., Wang, J.M. and Lanyi, J.K. (2005) Xanthorhodopsin: a proton pump with a light-harvesting carotenoid antenna. Science 309, 2061–2064.
[31] Brown, L.S. and Jung, K.H. (2006) Bacteriorhodopsin-like proteins of eubacteria and fungi: the extent of conservation of the haloarchaeal proton-pumping mechanism. Photochem. Photobiol. Sci. 5, 538–546.
[32] Bondar, A.N., Fischer, S., Suhai, S. and Smith, J.C. (2005) Tuning of retinal twisting in bacteriorhodopsin controls the directionality of the early photocycle steps. J. Phys. Chem. B 109, 14786–14788.
[33] Nachliel, E., Gutman, M., Kiryati, S. and Dencher, N.A. (1996) Protonation dynamics of the extracellular and cytoplasmic surface of bacteriorhodopsin in the purple membrane. Proc. Natl. Acad. Sci. U.S.A. 93, 10747–10752.
[34] Riesle, J., Oesterhelt, D., Dencher, N.A. and Heberle, J. (1996) D38 is an essential part of the proton translocation pathway in bacteriorhodopsin. Biochemistry 35, 66356643.
[35] Heberle, J. (2000) Proton transfer reactions across bacteriorhodopsin and along the membrane. Biochim. Biophys. Acta 1458, 135–147.
[36] Gerwert, K., Hess, B., Soppa, J. and Oesterhelt, D. (1989) Role of aspartate-96 in proton translocation by bacteriorhodopsin. Proc. Natl. Acad. Sci. U.S.A. 86, 4943–4947.
[37] Otto, H., Marti, T., Holz, M., Mogi, T., Lindau, M., Khorana, H.G. and Heyn, M.P. (1989) Aspartic acid-96 is the internal proton donor in the reprotonation of the Schiff base of bacteriorhodopsin. Proc. Natl. Acad. Sci. U.S.A. 86, 9228–9232.
[38] Joh, N.H., Min, A., Faham, S., Whitelegge, J.P., Yang, D., Woods, V.L. and Bowie, J.U. (2008) Modest stabilization by most hydrogen-bonded side-chain interactions in membrane proteins. Nature 453, 1266–1270.
[39] Muller, K.H., Butt, H.J., Bamberg, E., Fendler, K., Hess, B., Siebert, F. and Engelhard, M. (1991) The reaction cycle of bacteriorhodopsin – an analysis using visible absorption, photocurrent and infrared techniques. Eur. Biophys. J. 19, 241–251.
[40] Radu, I., Schleeger, M., Nack, M. and Heberle, J. (2011) Time-resolved FT-IR spectroscopy of membrane proteins. Aust. J. Chem. 64, 9–15.
[41] Abbruzzetti, S., Sottini, S., Viappiani, C. and Corrie, J.E. (2005) Kinetics of proton release after flash photolysis of 1-(2-nitrophenyl)ethyl sulfate (caged sulfate) in aqueous solution. J. Am. Chem. Soc. 127, 9865–9874.
[42] Brooks, B.R., Brooks III, C.L., Mackerell Jr., A.D., Nilsson, L., Petrella, R.J., Roux, B., Won, Y., Archontis, G., Bartels, C., Boresch, S., Caflisch, A., Caves, L., Cui, Q., Dinner, A.R., Feig, M., Fischer, S., Gao, J., Hodoscek, M., Im, W., Kuczera, K., Lazaridis, T., Ma, J., Ovchinnikov, V., Paci, E., Pastor, R.W., Post, C.B., Pu, J.Z., Schaefer, M., Tidor, B., Venable, R.M., Woodcock, H.L., Wu, X., Yang, W., York, D.M. and Karplus, M. (2009) CHARMM: the biomolecular simulation program. J. Comput. Chem. 30, 1545–1614.
[43] Kyte, J. and Doolittle, R.F. (1982) A simple method for displaying the hydropathic character of a protein. J. Mol. Biol. 157, 105–132.
[44] Notredame, C., Higgins, D.G. and Heringa, J. (2000) T-Coffee: a novel method for fast and accurate multiple sequence alignment. J. Mol. Biol. 302, 205–217.
[45] Poirot, O., Suhre, K., Abergel, C., O'Toole, E. and Notredame, C. (2004) 3DCoffee@igs: a web server for combining sequences and structures into a multiple sequence alignment. Nucleic Acids Res. 32, W37–W40.
[46] Humphrey, W., Dalke, A. and Schulten, K. (1996) VMD: visual molecular dynamics. J. Mol. Graph. 14, 33–38.
[47] Verhoefen, M.K., Bamann, C., Blocher, R., Forster, U., Bamberg, E. and Wachtveitl, J. (2010) The photocycle of channelrhodopsin-2: ultrafast reaction dynamics and subsequent reaction steps. Chemphyschem 11, 3113–3122.